

Intelligent self-monitoring and signal restoring system for the helicopter turboshaft engines gas temperature sensor with adaptive predicting^{*}

Serhii Vladov^{1,*†}, Victoria Vysotska^{2†}, Vasyl Lytvyn^{2†}, Nataliia Vladova^{3†} and Yelyzaveta Sahun^{3†}

¹ Kharkiv National University of Internal Affairs, L. Landau Avenue 27 61080 Kharkiv, Ukraine

² Lviv Polytechnic National University, Stepan Bandera Street 12 79013 Lviv, Ukraine

³ Ukrainian State Flight Academy, Chobanu Stepana Street 1 25005 Kropyvnytskyi, Ukraine

Abstract

In this research, an intelligent self-monitoring and signal restoring system for the helicopter turboshaft engine's gas temperature sensors based on adaptive predicting is developed. The system combines methods for the incoming signals' preliminary processing, anomaly detection based on comparative analysis of data from 14 dual thermocouples, and restoring of missing or distorted data using a modified LSTM network with dynamic stack memory and an adaptive outlier correction mechanism. The machine learning methods used allow for the expected signal values, short-term sensor failures, and accurate prediction prompt detection, which is critical for ensuring the helicopter operation's safety. Experimental modeling conducted in the MATLAB/Simulink environment confirmed the developed system's high efficiency, as evidenced by the root mean square error (RMSE = 0.622%), mean absolute error (MAE = 0.487%) low values, and high determination coefficient ($R^2 = 0.985$), as well as excellent classification accuracy indicators (Accuracy = 0.991, F1-score = 0.992). This approach opens up prospects for integration into onboard monitoring and diagnostics systems, ensuring continuous data transmission and increasing the engine operation reliability.

Keywords

Intelligent self-monitoring and signal restoring system, LSTM network, anomaly detection, gas temperature sensor, helicopter turboshaft engine

1. Introduction

In modern complex dynamic systems [1], including helicopter turboshaft engines (TE) [2], the measurement data reliability is a key factor in ensuring safety and operational efficiency. Modern sensors equipped with multiple measurement channels provide detailed information on operating parameters, but short-term failures or anomalies in their operation can lead to loss or distortion of data [3].

This topic relevance is due to the increasing requirements for the monitoring reliability and continuity the complex dynamic systems operation, where the multichannel sensors use (for example, on the TV3-117 engine [4], which is the Mi-8MTV helicopter power plant part [5], a sensor consisting of 14 dual thermocouples is used to record the gas temperature in front of the compressor turbine) ensures high measurement accuracy. Any failure or malfunction of the sensor can negatively affect the engine's diagnostics and operational management condition, which potentially leads to serious operational risks [6]. The machine learning and adaptive predicting methods use to restore missed or abnormal signals [7–9] not only increases the system's reliability,

^{*} CITI'2025: 3rd International Workshop on Computer Information Technologies in Industry 4.0, June 11–12, 2025, Ternopil, Ukraine

^{1*} Corresponding author.

[†] These authors contributed equally.

✉ serhii.vladov@univd.edu.ua (S. Vladov); victoria.a.vysotska@lpnu.ua (V. Vysotska); vasyi.v.lytvyn@lpnu.ua (V. Lytvyn); nataliia.vladova@sfa.org.ua (N. Vladova); yelyzavetasahun@sfa.org.ua (Y. Sahun)

ORCID: 0000-0001-8009-5254 (S. Vladov); 0000-0001-6417-3689 (V. Vysotska); 0000-0002-9676-0180 (V. Lytvyn); 0009-0009-7957-7497 (N. Vladova); 0000-0003-4837-4688 (Y. Sahun)



© 2025 Copyright for this paper by its authors. Use permitted under Creative Commons License Attribution 4.0 International (CC BY 4.0).

but also contributes to the intelligent technologies development in the aviation diagnostics field, which is an important step in improving the aviation equipment's safety and efficiency.

In this regard, the development of an intelligent self-monitoring and signal restoring system for an analog sensor based on adaptive predicting becomes necessary for prompt detection of faults and error correction in real time.

2. Related works

In recent decades, research in the sensor failure diagnostics and signal processing field has been actively developing. Many researches, for example [10–12], are devoted to the analog sensors under difficult operating conditions behavior analysis, which is especially relevant for helicopter TE, where the measuring systems reliability is critical. These researches often consider methods for detecting anomalies using statistical analysis and signal filtering, which allows for the deviations from normal sensor operation detection.

The digital technologies development has led to the intelligent analysis methods emergence, such as machine learning algorithms [13, 14] and neural networks [15, 16], used to predict the sensors and restore missing data state. Many researchers apply recurrent neural networks [17], ARIMA models [18], and adaptive filtering algorithms [19] to analyze time series, which allows predicting the parameters dynamics even under short-term failures. However, these approaches most are focused on digital sensors and systems with a redundancy high degree, and their application to analog sensors remains less researched.

Another research's significant aspect is the sensors self-diagnosis methods based methods on the several measurement channels comparative analysis [20]. The multiple sensors use for signal's cross-checking [19] can significantly increase the system's reliability. Despite this, existing studies, such as [19, 20], rarely pay attention to such methods integration with adaptive prediction algorithms that are not only detecting faults capable but also restoring data in real time.

Special attention is paid to the adaptive algorithms use to compensate for short-term sensor failures in aircraft equipment. Research in this area demonstrates the using Kalman filters possibility [21, 22], interpolation methods [23] and adaptive smoothing [24], but their effectiveness is limited in the complex engine dynamics conditions and the multiple correlating signals presence, as in the 14 dual thermocouples case. The improving such algorithms problem remains relevant to increase the data restoring systems accuracy and speed.

The need to address unsolved issues becomes especially obvious when considering the specifics of analog sensors installed on helicopter TEs. Existing methods often consider individual aspects – either diagnostics or data restoring, which leads to fragmented approaches. The integrated system lacks capable of simultaneously performing self-monitoring, fault detection, and prompt signal recovery indicates the need for further research in this area.

Thus, the intelligent self-monitoring and signal restoring system with adaptive predicting is a promising development direction that can combine the existing diagnostic, filtering and predicting methods achievements. The solution to this problem will improve the monitoring reliability the helicopter TE operation, ensure the data transmission continuity and, ultimately, improve the equipment operation safety.

The research objective is to develop an intelligent system for the analog sensor signals self-monitoring and restoring using adaptive predicting to improve the helicopter TE operation monitoring reliability. The research object is the helicopter TE measuring systems, in particular, temperature sensors consisting of 14 dual thermocouples installed on the TV3-117 engine. The research subject is the machine learning algorithms, adaptive predicting methods and digital signal processing integration for the faults prompt detection and missing data restoring under extreme operating conditions.

3. Materials and methods

3.1. Development of a system for restoring missing data in the short-term sensor failure case

The system proposed in the study (Figure 1) is based on the self-monitoring, adaptive predicting and signal restoring methods integration, which ensures the data coming from the analog sensor continuity and reliability. The machine learning algorithms and dynamic stack memory use for time series analysis and error correction ensures anomalies prompt detection and missing data restoring under extreme operating conditions.

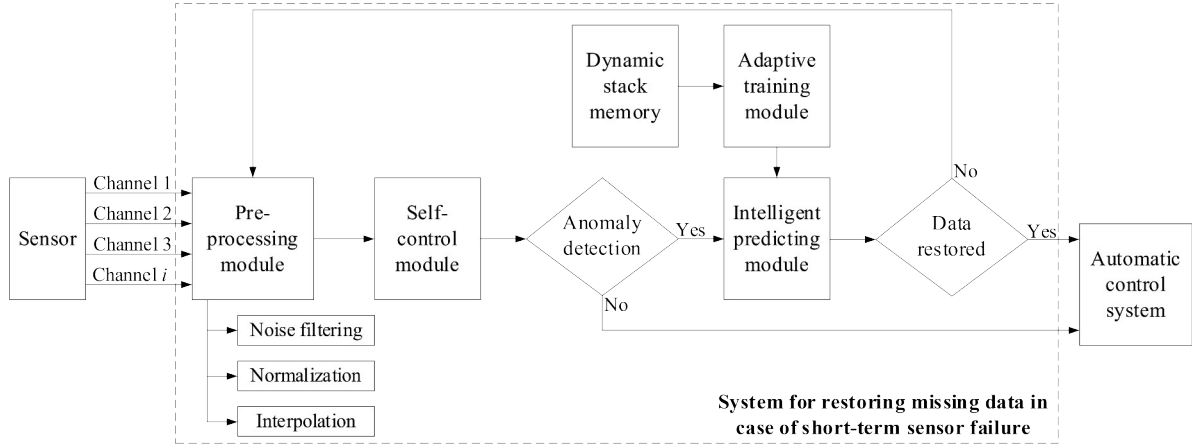


Figure 1: Block diagram of the proposed system for restoring missing data in short-term sensor failure case. (author's development).

The proposed system for restoring missing data in the short-term sensor failure event is implemented through the several functional blocks integration, which each performs its own specialized task in ensuring the measurement data reliability.

The self-monitoring module is responsible for epy incoming analog signals continuous monitoring from the gas temperature sensor installed on the engine (e.g., TV3-117). Using data comparative analysis from several channels (14 dual thermocouples), the system promptly detects anomalies or short-term failures, which allows for the failure timely detection or signal distortion.

The adaptive predicting module uses machine learning algorithms and time series analysis methods supported by dynamic stack memory. The module predicts the signal expected behavior based on historical data, which allows you to create the sensor operation adaptive model.

When deviations or omissions in data are detected, the signal restoring module performs error correction. Using interpolation, adaptive smoothing and other signal restoring algorithms, the module ensures the information continuity and reliability, compensating for short-term sensor failures.

Based on the above, an algorithm for the system's operation is proposed (Figure 1), ensuring the data continuity and reliability received from the analog sensor, due to the errors prompt detection and correction in real time (Table 1).

Table 1

The proposed algorithm for the system operation for restoring missing data in a short-term sensor failure case

| Number | Stage Name | Action |
|--------|-------------------------------|---|
| 1 | System initialization | 1. Loading operating parameters (sensor configuration, threshold values for anomaly detection, adaptive forecasting and signal restoring settings). 2. Initializing dynamic stack memory for storing historical measurement data. |
| 2 | Continuous data collection | 1. The system continuously receives analog signals from the gas temperature sensor (14 dual thermocouples installed on the TV3-117 engine). 2. Preliminary filtering and normalization of incoming data is performed to eliminate noise. |
| 3 | Self-monitoring procedure | A data comparative analysis from several channels is performed to identify deviations from normal operation: 1. If all measurements are within acceptable limits, the signal is passed to the next stage unchanged. 2. If short-term failures or anomalies are detected (e.g., a sharp drop/jump in signal, missing data), the corresponding sections are marked as faulty. |
| 4 | Adaptive prediction procedure | 1. When an anomaly is detected, the system accesses the predicting module, where the expected signal value is calculated using machine learning algorithms and time series analysis (using dynamic stack memory). 2. The predicted reliability degree value is assessed based on historical data and current measurement dynamics. |
| 5 | Signal restoring | 1. If the predicted value meets the reliability criteria, it is used to correct (restore) the missing or distorted signal. 2. If necessary, interpolation and adaptive smoothing are used to ensure a smooth transition between normal and restored sections. |
| 6 | Integration and data exchange | 1. The restored data is combined with the correct measurements into a single information flow. 2. Synchronous data exchange is provided between all system units for real-time operation. 3. The resulting signal is sent for the system's further monitoring and control, and is also saved in the event log for subsequent analysis. |
| 7 | Logging and status monitoring | 1. All events related to anomaly detection, predicts made and signal restoring are recorded in the system. 2. In critical deviations case, warnings are generated for the operator or automated decision-making system. |
| 8 | Cycle termination | After completing all steps, the system returns to the data collection stage, providing continuous monitoring of the sensor operation and prompt signal restoring in failures case. |

3.2. Development of a pre-processing module

The pre-processing module implements the incoming signal filtering and normalization received from the analog gas temperature sensor. It receives $x(t)$ is the analog signal, and after sampling is the $x[n] = x(n \cdot T)$, where T is the sampling period, n is the dataset's number.

To eliminate high-frequency components, a digital filter is used. Filtering is implemented by the input signal $x[n]$ convolution with the impulse response $h[k]$:

$$y[n] = \sum_{k=0}^{M-1} h[k] \cdot x[n-k], \quad (1)$$

where $y[n]$ is the filtered signal, M is the filter length, $h[k]$ are the filter coefficients. For example, for a simple moving average (MA filter [25]) with uniform weights

$$y[n] = \frac{1}{M} \cdot \sum_{k=0}^{M-1} x[n-k] \quad (2)$$

provides the input signal's smoothing by averaging values over a given interval.

After filtering, normalization is applied to eliminate bias and scale differences. To do this, the local mean and standard deviation are calculated over a window of L samples:

$$m[n] = \frac{1}{L} \cdot \sum_{i=n-L+1}^n y[i], \quad (3)$$

$$s[n] = \sqrt{\frac{1}{L-1} \cdot \sum_{i=n-L+1}^n (y[i] - m[n])^2}, \quad (4)$$

where $m[n]$ is the local mean, L is the averaging window length, $s[n]$ is the signal's standard deviation.

To bring the data to a single scale, z -normalization [26] is used, which removes bias and differences in the measurements scale, bringing the data to a standard normal distribution with a mean of 0 and a variance of 1:

$$z[n] = \frac{y[n] - m[n]}{s[n]}. \quad (5)$$

Thus, the preprocessing module performs an operations sequence:

1. Filtering noise by convolving the signal with a filter.
2. Calculating the local mean.
3. Estimating the standard deviation.
4. Normalizing the data to bring it to a standard scale.

As a result, a signal $z[n] = [z[1], z[2], \dots, z[N]]^T$ is formed, cleared of noise and prepared for subsequent processing (for example, anomaly detection and adaptive predicting).

3.3. Development of a self-monitoring module

The self-monitoring module analyzes incoming signals from an analog sensor. The module's main purpose is to detect anomalies, short-term failures or deviations from the sensor's normal operating mode. This research proposes a self-monitoring module mathematical model using the data example coming from 14 dual thermocouples of the gas temperature sensor installed on the TV3-117 engine.

We take $z_i[n]$ as the normalized measured temperature value for the i -th thermocouple at time n , where $i = 1, 2, \dots, 14$; $z[n] = \{z_1[n], z_2[n], \dots, z_{14}[n]\}$ is the normalized measurements vector from 14 thermocouples at time n ; $\bar{z}[n]$ is the average normalized temperature value for all thermocouples; $\sigma_z[n]$ is the normalized measurement's standard deviation:

$$\bar{z}[n] = \frac{1}{14} \cdot \sum_{i=1}^{14} z_i[n], \sigma_z[n] = \sqrt{\frac{1}{14} \cdot \sum_{i=1}^{14} (z_i[n] - \bar{z}[n])^2}. \quad (6)$$

Abnormal values are determined using the confidence interval:

$$Z_{min}[n] = \bar{z}[n] - k \cdot \sigma_z[n], Z_{max}[n] = \bar{z}[n] + k \cdot \sigma_z[n], \quad (7)$$

where k is the coefficient that determines the confidence limit level (usually $k = 3$, which corresponds to a 99.7 % confidence interval).

Measurements that go beyond the following limits are considered abnormal:

$$z_i[n] \notin [Z_{min}[n], Z_{max}[n]]. \quad (8)$$

The anomaly fact is recorded:

$$A[n] = \begin{cases} 1, \exists i: z_i[n] \notin [Z_{min}[n], Z_{max}[n]] \\ 0, otherwise \end{cases} \quad (9)$$

where $A[n] = 1$ means an anomaly was detected.

To eliminate random outliers, a sliding window of length L is used, in which the consecutive anomalies number is analyzed:

$$A_{sum}[n] = \sum_{j=n-L+1}^n A[j]. \quad (10)$$

If $A_{sum}[n]$ exceeds the A_{thr} threshold, a short-term failure is detected:

$$F[n] = \begin{cases} 1, A_{sum}[n] \geq A_{thr}, \\ 0, otherwise, \end{cases} \quad (11)$$

where $F[n] = 1$ means that the failure is confirmed.

The module produces three results:

1. Anomaly flag $A[n]$ means whether a deviation was detected in the current measurement.
2. Failure flag $F[n]$ means whether a short-term failure is detected in the interval L .
3. Anomaly channel array means a thermocouples list that are outside the confidence interval.

These data are passed to the adaptive forecasting module for subsequent signal restoring.

3.4. Development of an adaptive predicting module

3.4.1. Development of a modified LSTM network with dynamic stack memory

The adaptive predicting module is designed to restore missing or distorted signals from helicopter TE gas temperature sensors. For this purpose, it is proposed to use a modified LSTM network with dynamic stack memory [27–30] (Figure 2).

The classical LSTM network [27, 28] effectively processes time series, taking into account long-term dependencies, but has disadvantages such as high computational costs, sensitivity to noise in the data, and a fixed input window size, which reduces the efficiency when analyzing signals with variable dynamics. The proposed modified LSTM network with a dynamic stack memory and an

adaptive anomaly processing mechanism provides more robust and efficient operation, especially in real time as an onboard monitoring and parameter recording systems part.

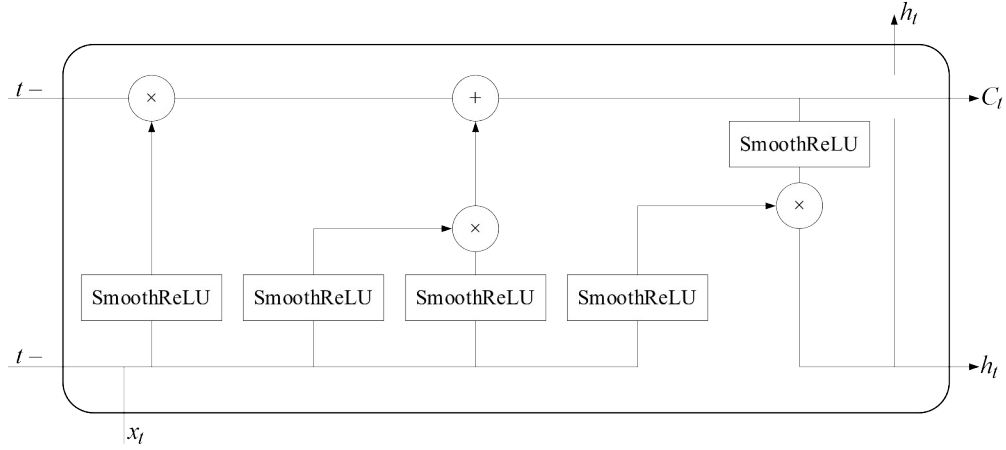


Figure 2: The modified LSTM network with dynamic stack memory architecture. (author's development).

Key changes include the dynamic stack memory [31] addition, which efficiently manages context information, reducing the standard LSTM cells overhead and accelerating time series processing through optimal data storage and retrieval. Adaptive Anomaly-Adaptive LSTM (AA-LSTM) [32] implements a mechanism for adjusting input data based on the predicted confidence boundary, minimizing the outlier's impact on prediction. In addition, a modified SmoothReLU [33] is used the standard sigmoid and tangent-hyperbolic activation functions instead:

$$f(x) = \begin{cases} x, & \text{if } x > 0, \\ \frac{1}{1 + e^{-\gamma \cdot x}}, & \text{if } x \leq 0. \end{cases} \quad (12)$$

In (12), the parameter γ specifies the function “smoothness” degree. For $x > 0$, it works the same as the traditional ReLU, and for $x \leq 0$, a smooth transition to negative values occurs via a sigmoid transformation. This mechanism prevents sharp jumps in the gradient, which can help speed up the neural network's training process. The SmoothReLU activation function preserves the traditional ReLU positive aspects, such as a zero gradient for positive input values, while providing smoother behavior for negative values [33]. Also, in [33], a theorem on the SmoothReLU function continuity in the definition's entire domain is formulated and proven. In this case, a parametric threshold is set that increases the model's accuracy and stability:

$$f(x) = \max(\alpha \cdot x, \beta \cdot \tanh(x)). \quad (13)$$

The modified LSTM basic equations include the input block, forget block, state update block, and output block equations:

$$\begin{aligned} i_t &= \text{SmoothReLU}(W_i \cdot [z_t, h_{t-1}] + b_i), f_t = \text{SmoothReLU}(W_f \cdot [z_t, h_{t-1}] + b_f), \\ \tilde{C}_t &= \text{SmoothReLU}(W_c \cdot [z_t, h_{t-1}] + b_c), C_t = f_t \odot C_{t-1} + i_t \odot \tilde{C}_t, \\ o_t &= \text{SmoothReLU}(W_o \cdot [z_t, h_{t-1}] + b_o), h_t = o_t \odot \text{SmoothReLU}(C_t), \end{aligned} \quad (14)$$

where W_i, W_f, W_c, W_o are weight matrices, b_i, b_f, b_c, b_o are biases, \odot is component-wise multiplication.

The introduced dynamic stack memory (Figure 3) allows to consider only the most significant the hidden layer states h_t . Instead of storing all C_t , a stack S is used, where:

$$S_t = \text{push}(C_t, S_{t-1}), \quad (15)$$

where $\text{push}(C_t, S_{t-1})$ is the adding a new state to the stack operation, and excess elements are removed:

$$S_t = \{C_t, C_{t-1}, \dots, C_{t-T_s+1}\}, \quad (16)$$

where T_s is the maximum stack size.

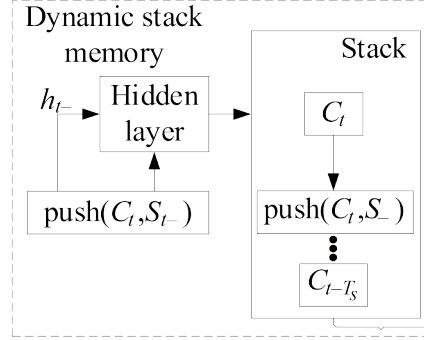


Figure 3: The dynamic stack memory structural diagram. (author's development).

The dynamic stack memory implemented in the developed modified LSTM network (Figure 2), which limits the stored states number to the most significant T_s , allows to reduce computational costs and improve the predicting quality due to effective information management under conditions of variable signal dynamics.

For the modified LSTM network adaptive training [34], the error function minimization, for example, the mean square error (MSE) between the normalized signals predicted and true values is used as:

$$L(\theta) = \frac{1}{N} \cdot \sum_n (z[n+1] - \hat{y}[n+1])^2. \quad (17)$$

Training is performed using the backpropagation over time (BPTT) method with updating the θ parameters [35]. In this case, a dynamic stack memory helps to preserve the most relevant information, and an adaptive input data correction mechanism (using SmoothReLU and the threshold mechanism (12)–(13)) reduces the anomalous emissions impact on the training process.

3.4.2. Development of a model for an adaptive predicting module

The adaptive control module performs prediction $\hat{z}[n]$ based on the previous values of a given time series $z[n]$ of normalized parameter values coming from an analog sensor. Thus, the input data for the developed LSTM network (Figure 2) are represented as:

$$Z = [z[n-T], z[n-T+1], \dots, z[n]]^T, \quad (18)$$

where T is the time window length.

Then the model's output is represented as:

$$\hat{z}[n+1] = f(Z, \theta), \quad (19)$$

where θ are the trained LSTM network's parameters.

The predicted value is calculated as:

$$\hat{z}[n+1] = W_{ij} \cdot h_t + b_{ij}, \quad (20)$$

The final reconstructed value $\hat{x}[n+1]$ is obtained by inverse normalization as:

$$\hat{x}[n+1] = \hat{z}[n+1] \cdot s[n] + m[n], \quad (21)$$

where $s[n]$ and $m[n]$ are the previously calculated standard deviation and mean.

4. Results

4.1. Development of an adaptive predicting module

The research conducted a computational experiment, which results confirm the developed system's (Figure 1) operability. For this purpose, a gas temperature sensor, consisting of 14 dual thermocouples T-102, short-term failure simulation modeling was carried out. To carry out the simulation modeling, a simulation modeling stand was developed (Figure 4) consisting of a software and hardware complex in which the researched sensor input signals are simulated.

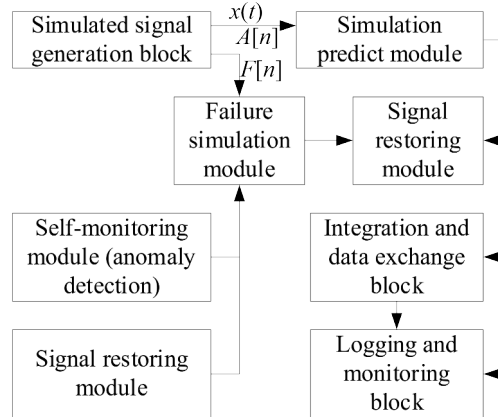


Figure 4: The developed simulation modeling stand's structural scheme. (author's development).

The simulated signal generation block creates synthetic time series simulating the normal behavior of 14 dual thermocouples that are simultaneously fed to the failure simulation module. It allows basic parameters such as mean and variance to be specified, as well as noise modeling, corresponding to the analog signal $x(t)$ and its sampling $x[n]$.

The failure simulation module introduces artificial short-term failures (anomalies) into the simulated signals. It supports parameterizable failure scenarios such as spikes, drops, and data gaps, which allows testing the anomaly detection algorithms described in (7)–(11).

The preprocessing module filters and normalizes the incoming signals using a digital filter (convolution with the impulse response $h[k]$ according to (1)) and z-normalization (see (3)–(5)). The final result is a signal cleared of noise, ready for further analysis.

The self-monitoring (anomaly detection) module analyzes the normalized data to detect anomalies and short-term failures through comparative analysis of 14 channels. It calculates the mean and standard deviation according to (6) and determines the anomaly flags $A[n]$ and failure flags $F[n]$ according to (7)–(11).

The adaptive prediction module predicts the expected value of a signal when an anomaly is detected using a modified LSTM network with dynamic stack memory and an adaptive anomaly

processing mechanism. It takes as input a window of T normalized data samples according to (17) and outputs the predicted value $\hat{y}[n+1]$ according to (18)–(20).

The signal restoration module corrects and restores missing or corrupted data based on the predicted value. It uses interpolation and adaptive smoothing to ensure a smooth transition between normal and restored signal sections.

The integration and data exchange unit combines the restored data with the correct measurements and ensures synchronous information exchange between all modules. It forms a single data stream for subsequent monitoring and system control.

The logging and monitoring unit records all events, including detected anomalies, predicting triggering and restoring modules, and critical deviations. It displays information in real time on the operator visualization panel and saves it to a log for subsequent analysis.

Based on the logging data, by introducing feedback, it is possible to adjust the simulation parameters (e.g., the failure's duration and intensity) and processing settings, which allows optimizing the system algorithms under testing conditions.

The MATLAB/Simulink 2014b software environment with the corresponding libraries (Figure 5) was used as a platform for the simulation modeling stand. This implementation ensures the synthetic signals generation, failure scenarios control, detection operation and restoring algorithms, as well as data visualization and analysis in real time.

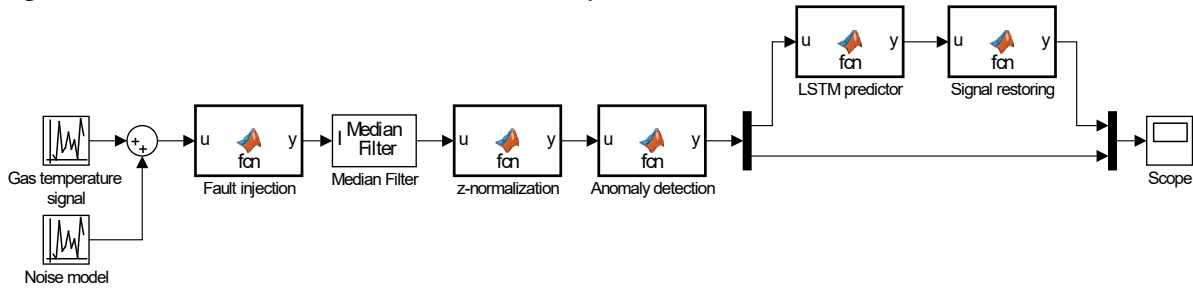


Figure 5: The developed simulation modeling stand scheme, implemented in the MATLAB/Simulink 2014b software environment. (author's development).

The signal generator (gas temperature signal and noise model) module creates synthetic input signals for 14 dual thermocouples, which are subjected to random noise, and then passed to the Fault Injection module via MATLAB Function to introduce specified anomalies (sharp jumps, zeros, data gaps). The preprocessing module filters (median filter) and z-normalizes the signals, preparing them for analysis in the anomaly detection module, where the mean value and standard deviation are calculated to detect anomalies. Based on the normalized data, the LSTM predictor module, using a modified LSTM network, predicts the next sample's expected value, which allows the signal-restoring module to correct the detected failures, replacing corrupted or missing data with predicted values. The integration and logging module (Mux, Scope) combines the restored data and displays the results in real time, ensuring synchronous information exchange for further analysis.

The MATLAB Function block is also used to implement the self-monitoring module (anomaly detection) in MATLAB/Simulink. This module takes as input a normalized gas temperature values vector from 14 dual thermocouples, calculates their mean value and standard deviation according to (6), determines the confidence interval with the coefficient k (usually $k = 3$, see (7)) and sets the anomaly flag $A[n]$ for channels where the measurement goes beyond its limits (see (8)–(9)).

4.2. The input data description and preprocessing

According to the authors' collective official request to the Ministry of Internal Affairs of Ukraine within the research project "Theoretical and applied aspects of aviation sphere development" framework (no. 0123U104884), the Mi-8MTV helicopter flight tests data, which power plant includes the TV3-117 engine, were received. It is noted that the tests were carried out at the nominal engine operating mode at a flight altitude of 2500 meters above sea level. To conduct the

simulation modeling, the engine's gas temperature in front of the compressor turbine T_G^* values were used, recorded by the standard onboard monitoring system for 320 seconds with a sampling interval of 0.25 seconds [36, 37].

In the interval from 225 to 235 seconds, adjustments were made by equating the recorded values of T_G^* to zero, simulating a short-term failure of the temperature sensor (Figure 6). Thus, in the T_G^* dynamics research 320-second interval, this parameter's 40 values are missing.

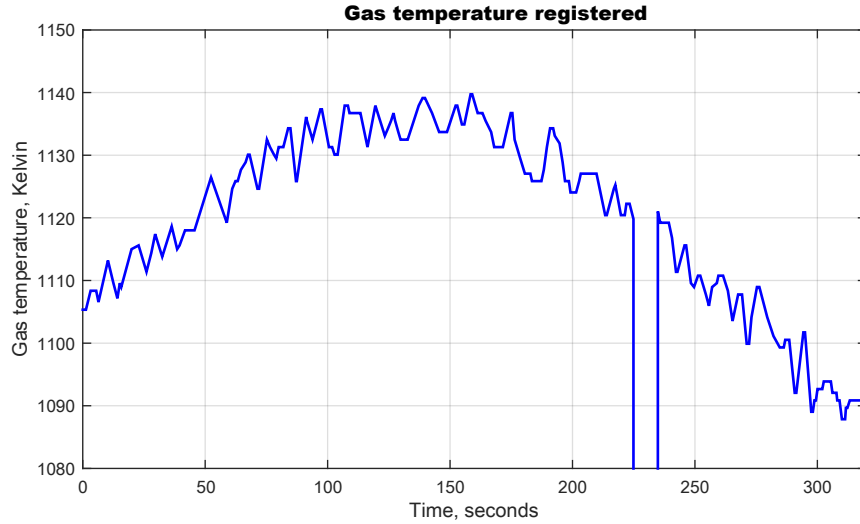


Figure 6: Diagram of the change in the gas temperature in front of the compressor turbine dynamics over a 320-second research interval with a gas temperature sensor short-term failure in the period from 225 to 235 seconds. (author's development).

The initial data (Figure 6) were subjected to primary processing in the pre-processing module (see subsection 3.2) with the noise interference elimination, after which they were transformed into time series is the parameters sets organized by time scale. To ensure time series comparability with parameters different scales, z -normalization was used, normalizing their values to a single range, shifting the mean to zero and setting the standard deviation equal to one. This allowed us to form the parameter T_G^* training dataset, which fragment is presented in Table 2.

Table 2

Training dataset fragment

| | | | | | | | | | |
|---------------------------|--------|-----|--------|-----|--------|-----|--------|-----|--------|
| Number | 0 | ... | 50 | ... | 100 | ... | 150 | ... | 200 |
| T_G^* | 1105.3 | ... | 1123.5 | ... | 1131.7 | ... | 1135.6 | ... | 1124.2 |
| Number | ... | 225 | ... | 230 | ... | 235 | ... | ... | 320 |
| T_G^* | ... | 0 | ... | 0 | ... | 0 | ... | ... | 1090.6 |

As can be seen from Table 2, in the interval from 225 to 235 seconds, the values are zero, which indicates the temperature sensor's short-term failure. This indicates the anomalous data presence in the training dataset. At the pre-processing stage, it is impossible to objectively assess the training dataset homogeneity, since it contains anomalous data that distort the dataset's statistical characteristics. Such anomalies' presence leads to a shift in the features' distribution, which complicates the determination of their consistency and violates the correct data partitioning principles degree [38–40]. Therefore, to ensure the subsequent analysis and the model training reliability, it is necessary to pre-identify and restore distorted or missing values, eliminating their influence on the training process. At the same time, Table 3 shows the self-monitoring module results, which confirmed the temperature sensor's short-term failure in the interval from 225 to 235 seconds.

Table 3

The self-monitoring module results, according to (11)

| | | | | | | | | | |
|--------------------------|-----|-----|-----|-----|-----|-----|-----|-----|-----|
| Number | 225 | ... | 226 | ... | 227 | ... | 228 | ... | 229 |
| $F[n]$ | 1 | ... | 1 | ... | 1 | ... | 1 | ... | 1 |
| Number | ... | 230 | ... | 231 | ... | 232 | ... | ... | 235 |
| $F[n]$ | ... | 1 | ... | 1 | ... | 1 | ... | ... | 1 |

4.3. The simulation modeling results

In the simulation modeling, the modified LSTM network with dynamic stack memory and adaptive anomaly processing mechanism (Figure 2) restored the anomalous data (Figure 7), where the blue curve shows the original data with the temperature sensor normal functioning, recorded during helicopter flight; the red curve shows the data restored by the modified LSTM network. The results presented in Figure 7 demonstrate successful restoration of the anomalous data by the modified LSTM network with dynamic stack memory with the temperature sensor short-term failure at a 225...235 seconds interval. It is evident that the model correctly interpolated the missing values, providing a smooth transition between normal and restored signal sections.

As can be seen from Figure 7, the T_G^* signal characteristic dynamics smooth restoring and preservation (the restored T_G^* values are in the acceptable range from 1080 to 1150 Kelvin) confirm that the model effectively adapts to changes in the sensor parameters, which is critical for the failure's timely diagnostics and prevention in real time. The conducted simulation modeling results confirmed the compensating effectiveness for short-term sensor failures due to the modified LSTM network use.

Table 4 shows the anomalous data restoring quality evaluation results by the modified LSTM network using traditional quality metrics. The root mean square error (RMSE) and mean absolute error (MAE) allow us to quantitatively evaluate the model deviations from the experimental data, and the determination coefficient (R^2) characterizes the explained variance degree, demonstrating how well the model describes the experimental results [40, 41]. In Table 4, $(T_G^*)_{pred}^{(i)}$ means the gas temperature predicted value by the modified LSTM network, $(T_G^*)_{real}^{(i)}$ means the gas temperature real value recorded on board the helicopter in flight mode, and the gas temperature average value recorded on board the helicopter at flight mode.

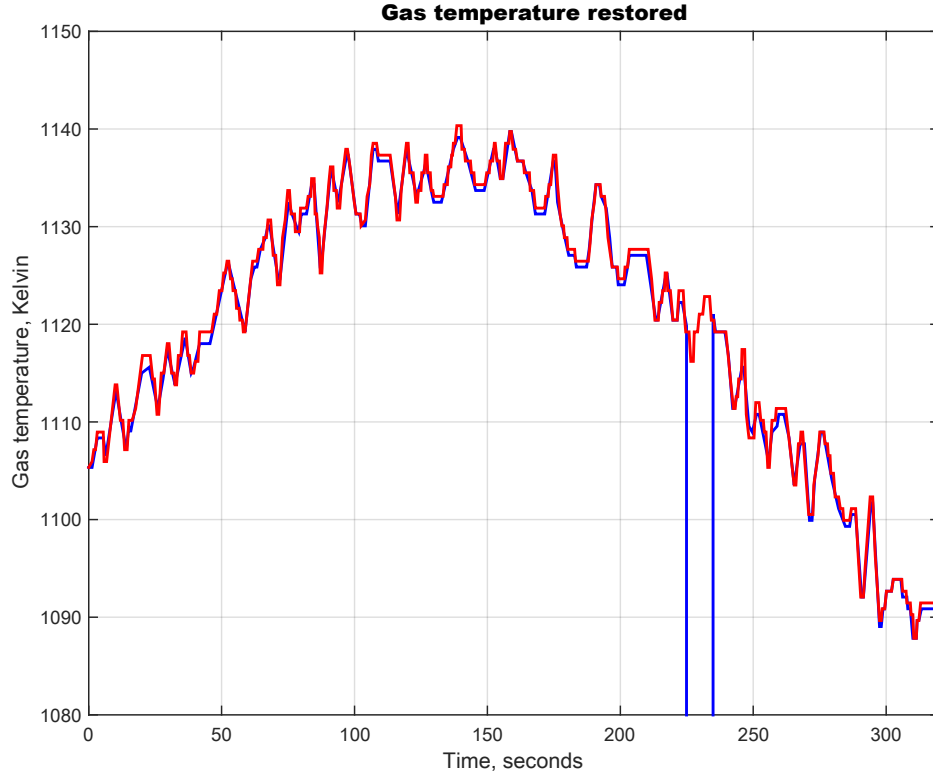


Figure 7: Results of restoring abnormal data from a short-term temperature sensor failure. (author's development).

Table 4

The data restoring quality in case of the temperature sensor short-term failure assessing results

| Metric | Analytical expression | Resulting value |
|-------------------------------------|--|-----------------|
| Root Mean Square Error (RMSE, %) | $RMSE = \sqrt{\frac{1}{N} \cdot \sum_{i=1}^N \left((T_G^*)_{pred}^{(i)} - (T_G^*)_{real}^{(i)} \right)^2}$ | 0.622 |
| Mean Absolute Error (MAE, %) | $MAE = \frac{1}{N} \cdot \sum_{i=1}^N \left (T_G^*)_{pred}^{(i)} - (T_G^*)_{real}^{(i)} \right $ | 0.487 |
| Determination Coefficient (R^2) | $R^2 = 1 - \frac{\frac{1}{N} \cdot \sum_{i=1}^N \left((T_G^*)_{pred}^{(i)} - (T_G^*)_{real}^{(i)} \right)^2}{\frac{1}{N} \cdot \sum_{i=1}^N \left((T_G^*)_{real}^{(i)} - (\bar{T}_G^*) \right)^2}$ | 0.985 |

Table 5 shows the modified LSTM network training results average values, as well as the accuracy indicator mean and variance values, where TP denotes the signals, the number correctly restored by the model, TN is the cases number when the signal is correctly left unchanged, FP is the signals number mistakenly accepted as requiring restoration, and FN is the cases when the model did not detect the need for restoration and skipped restoring the distorted signal.

Table 5

The data restoring quality in the temperature sensor short-term failure case assessing results

| Metric | Analytical expression | Resulting value |
|-----------------------|---|-----------------|
| Accuracy | $Accuracy = \frac{TP + TN}{TP + TN + FP + FN}$ | 0.991 |
| Precision | $Precision = \frac{TP}{TP + FP}$ | 0.985 |
| Recall | $Recall = \frac{TP}{TP + FN}$ | 0.999 |
| F1-score | $F1\text{-score} = 2 \cdot \frac{Precision \cdot Recall}{Precision + Recall}$ | 0.992 |
| Average time, seconds | – | 217 |
| Average Accuracy | $\bar{A} = \frac{1}{N} \cdot \sum_{i=1}^N A_i$ | 0.990 |
| Dispersion Accuracy | $D_A = \frac{1}{N} \cdot \sum_{i=1}^N (A_i - \bar{A})^2$ | 0.00000094 |

The results presented in Table 4 confirm the proposed model's high efficiency for restoring abnormal temperature sensor data. The root mean square error (RMSE = 0.622%) and mean absolute error (MAE = 0.487%) low values indicate the reconstructed values' minimal deviations from the real data, which indicates the neural network model's accuracy. The high determination coefficient ($R^2 = 0.985$) demonstrates that the original data variance model explains 98.5%, which confirms its ability to accurately predict missing values.

The metrics presented in Table 5 show that the modified LSTM network has high classification accuracy (Accuracy = 0.991), as well as balanced Precision (Precision = 0.985) and Recall (Recall = 0.999) values, which indicates its ability to effectively detect anomalies without a significant number of false positives. The high F1-score (F1-score = 0.992) confirms the model's reliability in real-world conditions. The low Dispersion Accuracy value (Dispersion Accuracy = 0.00000094) indicates the predictions' stability, and the 217 seconds average running time makes it possible to apply the model to the data restoring practical problems in the helicopter TE on-board monitoring systems [42].

Thus, the proposed model demonstrated high efficiency in restoring abnormal data and identifying short-term failures of the helicopter TE temperature sensor. The experimental results confirm its stability, accuracy and applicability in real-time conditions, which makes it promising for integration into the helicopter TE intelligent self-monitoring and diagnostic systems.

5. Discussion

5.1. The obtained results analysis

This research presents a comprehensive approach to restoring missing data from transient sensor failures. The proposed methods are for pre-processing the incoming signals: filtering is performed using convolution (1) and subsequent normalization, where the local mean and standard deviation (3)–(5) are calculated. The self-monitoring module, implemented according to (6)–(11) and illustrated in Figure 1, performs a comparative analysis of data from 14 dual thermocouples to detect anomalies and record transient failures.

An adaptive forecasting module based on a modified LSTM network with a dynamic stack memory has been developed, as demonstrated in Figure 2. The development novelty lies in the dynamic stack memory integration (15)–(16) for storing the most significant states and the modified SmoothReLU activation function (12) use, which allows increasing the model's resistance to noise and sharp jumps in the data. This approach ensures not only accurate forecasting (17)–(21) but also prompt signal restoring, which is a significant contribution to the helicopter TE monitoring and diagnostics systems development.

The gas temperature sensor signals self-monitoring and restoring developed system operability experimental verification was carried out. As the research part, a temperature sensor short-term failure simulation modeling consisting of 14 dual thermocouples was carried out, followed by the modified LSTM network use for data restoring. The original and restored data visual comparison is presented in Figure 7, which demonstrates the model's high accuracy (99.1%) in the presence of the missing or distorted signals.

The proposed method's efficiency quantitative assessment is presented in Table 4, where the root mean square error (RMSE = 0.622%) and mean absolute error (MAE = 0.487%) low values, as well as a high determination coefficient ($R^2 = 0.985$), are recorded, which indicates a minimal discrepancy between the predicted and actual values. At the same time, Table 5 shows the model quality indicators, including classification accuracy (Accuracy = 0.991) and F1-score = 0.992, which confirms its reliability in detecting and restoring anomalous data. Thus, the proposed system demonstrated high efficiency in identifying short-term failures and restoring missing values, which makes it promising for integration into on-board helicopter TE monitoring systems.

5.2. Evaluation of the modified LSTM network with dynamic stack memory effectiveness in a self-monitoring and signal restoring system for a gas temperature sensor

To evaluate the modified LSTM network with dynamic stack memory (Figure 2) efficiency used to reconstruct temperature sensor signals under short-term failure conditions, two key metrics were used: the efficiency coefficient and the quality coefficient. The efficiency coefficient (K_{eff}) evaluates the modified LSTM network training efficiency and is defined as the change ratio in the loss function at the current iteration to the change in the network parameters at the same iteration; this metric allows us to determine how quickly and adequately the network adapts to errors during the optimization process. The quality coefficient ($K_{quality}$), in turn, evaluates the modified LSTM network parameters' approximation accuracy and is defined as the decrease ratio in the loss function at the current iteration to the total loss function at previous iterations, which reflects the model's stability and convergence during the training process. Together, these metrics provide the modified LSTM network efficiency comprehensive assessment, facilitating its training characteristics objective analysis and the signal reconstruction accuracy. The efficiency and quality coefficients are calculated as [43]:

$$K_{eff} = \frac{|E(\theta_k) - E(\theta_{k-1})|}{\|\theta_k - \theta_{k-1}\|}, K_{quality} = \frac{E(\theta_{k-1}) - E(\theta_k)}{E(\theta_0) - E(\theta_{k-1})}, \quad (22)$$

where $E(\theta_0)$ is the loss function initial value, $E(\theta_k)$ is the loss function value at the current iteration, $E(\theta_{k-1})$ is the loss function value at the previous iteration, $\|\theta_{k-1} - \theta_k\|$ is the modified LSTM network parameters change rate at the current iteration.

Table 6 presents a reconstructing signals efficiency comparative analysis from the helicopter TE gas temperature in front of the compressor turbine sensor using a modified LSTM network, as well as other traditional recurrent neural network architectures adapted to similar problems: traditional LSTM network [44], traditional GRU network [45], and traditional RNN network [46].

Table 6

The helicopter TE gas temperature in front of the compressor turbine sensor signal restoring efficiency comparative analysis results

| The recurrent neural network architecture | Efficiency coefficient (K_{eff}) | Quality coefficient ($K_{quality}$) |
|---|--------------------------------------|---------------------------------------|
| Modified LSTM network | 0.991 | 0.989 |
| Traditional LSTM network [44] | 0.982 | 0.977 |
| Traditional GRU network [45] | 0.965 | 0.960 |
| Traditional RNN network [46] | 0.943 | 0.938 |

As can be seen from Table 6, the modified LSTM network showed the 0.991 and 0.989 values, which indicate an adaptive predicting and model approximation accuracy high level. Compared with the traditional LSTM network (0.982 and 0.977), the modified LSTM network shows an increase of about 0.9 % in efficiency and about 1.2 % in quality, and when compared with the traditional GRU network (0.965 and 0.960), the improvement is about 2.7 % in efficiency and 3.0% in quality. The most noticeable advantage is observed compared to the traditional RNN network, where the 0.943 and 0.938 values indicate an improvement of about 5.1 and 5.4 %, respectively. Even minor improvements in efficiency and quality factors are critical because in helicopter TE operating conditions, where safety and reliability are a priority, the slightest increase in signal recovery accuracy significantly reduces the system failures risk [47, 48]. Such percentages can be critical in high-risk scenarios, where each unit of accuracy prevents potentially catastrophic consequences.

5.3. Limitations and prospects for further research

Despite the high accuracy of signal recovery (RMSE = 0.622 %, MAE = 0.487 %, $R^2 = 0.985$) and reliable anomaly detection (Accuracy = 0.991, F1-score = 0.992), the system has certain limitations. Moreover, the experimental evaluation was carried out under simulation modeling conditions, which requires further verification on real flight test data to ensure the model stability under changing operating conditions and noise levels. In addition, the modified LSTM network high computational complexity with dynamic stack memory and the need for fine-tuning of parameters (e.g., anomaly detection thresholds and memory sizes) may limit the system use in real-time onboard conditions.

It is also noted that the various modules integration (pre-processing, anomaly detection, adaptive predicting and signal restoration) requires deeper optimization to reduce computational costs and increase stability under extreme operating conditions. The expanding algorithms task to handle various failure scenarios, such as long-term failures or systematic deviations, also remains relevant, which opens up prospects for further research and improvements to the system.

Based on the presented limitations, Table 7 provides directions for further research, actions and expected end results.

Table 7

Roadmap for future research

| Direction | Action | Final result |
|--|--|---|
| Optimizing computational efficiency | Development of LSTM parameters simplified algorithms and optimization [49, 50] | Reducing the computational load and accelerating the system operation |
| Expanding testing | Conducting experiments on real data (helicopter TE tests) [51, 52] | Confirming the system's reliability in real flight conditions |
| Improving anomaly detection algorithms | Integration of additional filtering methods [53, 54] and adaptive threshold adjustment [55–60] | Increasing the signal detection and restoring accuracy in various failure cases |

6. Conclusions

An intelligent system for the helicopter TE temperature sensor self-monitoring and signal restoring has been developed, which combines preliminary processing, anomaly detection, and adaptive predicting methods. The development novelty lies in the modified LSTM network with a dynamic stack memory integration and an adaptive anomaly processing mechanism, which allows not only to detect short-term failures in the sensors' operation but also to quickly restore missing or distorted data.

The obtained simulation results confirm the proposed system's effectiveness: the reconstructed signals demonstrate minimal deviations from the reference values (RMSE = 0.622 %, MAE = 0.487 %, $R^2 = 0.985$), and the classification metrics indicate high accuracy in anomaly detection (Accuracy = 0.991, F1-score = 0.992). These indicators indicate that the dynamic stack memory and adaptive predicting significantly improve the time series processing quality, allowing the system to operate in real time and ensure continuous data transmission.

Thus, the conducted study demonstrates that the proposed approach is effectively capable of compensating for short-term sensor failures under helicopter TE extreme operating conditions, which is of great practical importance for improving the equipment's operation safety and reliability. The developed approaches and high signal restoring quality novelty indicators open up prospects for the system's further adaptation and integration into real onboard monitoring systems, as well as for expanding its application in other areas requiring accurate and rapid analysis of dynamic processes.

Acknowledgements

The research was carried out with the grant support of the National Research Fund of Ukraine "Methods and means of active and passive recognition of mines based on deep neural networks", project registration number 273/0024 from 1/08/2024 (2023.04/0024). This research also was supported by the Ministry of Education and Science of Ukraine "Methods and means of identification of combat vehicles based on deep learning technologies for automated control of target distribution" under Project No. 0124U000925 and by the Ministry of Internal Affairs of Ukraine "Theoretical and applied aspects of the development of the aviation sphere" under Project No. 0123U104884. Also, we would like to thank the reviewers for their precise and concise recommendations that improved the presentation of the results obtained.

Declaration on Generative AI

The authors have not employed any Generative AI tools.

References

- [1] M. Li, Y. Luo, L. Qu, L. Xie, B. Zhao, Influence of ring gear flexibility on the fatigue reliability of planetary gear systems in heavy helicopters, *Mechanism and Machine Theory* 191 (2024) 105520. doi: 10.1016/j.mechmachtheory.2023.105520.
- [2] T. Castiglione, D. Perrone, J. Song, L. Strafella, A. Ficarella, S. Bova, Linear model of a turboshaft aero-engine including components degradation for control-oriented applications, *Energies* 16:6 (2023) 2634. doi: 10.3390/en16062634.
- [3] H. Aygun, Effects of air to fuel ratio on parameters of combustor used for gas turbine engines: Applications of turbojet, turbofan, turboprop and turboshaft. *Energy* 305 (2024) 132346.
- [4] S. Vladov, L. Scislo, V. Sokurenko, O. Muzychuk, V. Vysotska, A. Sachenko, A. Yurko, Helicopter Turboshaft Engines' Gas Generator Rotor R.P.M. Neuro-Fuzzy On-Board Controller Development, *Energies*, 17:16 (2024), 4033. doi: 10.3390/en17164033.
- [5] A. de Voogt, E. St. Amour, Safety of Twin-Engine Helicopters: Risks and Operational Specificity. *Safety Science* 136 (2021) 105169. doi: 10.1016/j.ssci.2021.105169.

- [6] P. Kurdel, A. Novák, A. N. Sedláčková, L. Korba, The Methods of Helicopter Control in Non-standard Situations, *Transportation Research Procedia* 59 (2021) 214–222.
- [7] S. Vladov, V. Vysotska, V. Sokurenko, O. Muzychuk, M. Nazarkevych, V. Lytvyn, Neural Network System for Predicting Anomalous Data in Applied Sensor Systems, *Applied System Innovation* 7:5 (2024) 88. doi: 10.3390/asi7050088.
- [8] S. Yepifanov, O. Bondarenko, Development of Turboshift Engine Adaptive Dynamic Model: Analysis of Estimation Errors, *Transactions on Aerospace Research* 2022:4 (2022) 59–71.
- [9] S. Yepifanov, O. Bondarenko, Forming of turboshift engine mathematical model, *Aerospace Technic and Technology* 4sup1 (2023) 85–94. doi: 10.32620/akt.2023.4sup1.12.
- [10] O. Lytviak, V. Loginov, S. Komar, Y. Martseniuk, Self-Oscillations of The Free Turbine Speed in Testing Turboshift Engine with Hydraulic Dynamometer, *Aerospace* 8:4 (2021) 114.
- [11] S. J. Mohammadi, S. A. M. Fashandi, S. Jafari, T. Nikolaidis, A scientometric analysis and critical review of gas turbine aero-engines control: From Whittle engine to more-electric propulsion, *Measurement and control* 54:5–6 (2021) 935–966. doi: 10.1177/0020294020956675.
- [12] Y. Wang, C. Cai, J. Song, H. Zhang, An optimal speed control method of multiple turboshift engines based on sequence shifting control algorithm, *Journal of Dynamic Systems, Measurement, and Control* 144:4 (2022) 041003. doi: 10.1115/1.4053088.
- [13] H. Chen, Q. Li, Z. Ye, S. Pang, Neural Network-Based Parameter Estimation and Compensation Control for Time-Delay Servo System of Aeroengine, *Aerospace* 12:1 (2025) 64.
- [14] A. Aghazadeh Ardebili, A. Ficarella, A. Longo, A. Khalil, S. Khalil, Hybrid Turbo-Shaft Engine Digital Twinning for Autonomous Aircraft via AI and Synthetic Data Generation, *Aerospace* 10:8 (2023) 683. doi: 10.3390/aerospace10080683.
- [15] S. Vladov, Y. Shmelov, M. Petchenko. A Neuro-Fuzzy Expert System for the Control and Diagnostics of Helicopters Aircraft Engines Technical State, *CEUR Workshop Proceedings* 3013 (2021) 40–52. URL: <https://ceur-ws.org/Vol-3013/20210040.pdf>
- [16] S. Vladov, Y. Shmelov, R. Yakovliev, Y. Stushchankyi, Y. Havryliuk, Neural Network Method for Controlling the Helicopters Turboshift Engines Free Turbine Speed at Flight Modes, *CEUR Workshop Proceedings* 3426 (2023) 89–108. URL: <https://ceur-ws.org/Vol-3426/paper8.pdf>
- [17] S. Vladov, Y. Shmelov, R. Yakovliev, Optimization of Helicopters Aircraft Engine Working Process Using Neural Networks Technologies, *CEUR Workshop Proceedings* 3171 (2022) 1639–1656. URL: <https://ceur-ws.org/Vol-3171/paper117.pdf>
- [18] M. Mary Victoria Florence, E. Priyadarshini, Aeroengine gas trajectory prediction using time-series analysis auto regressive integrated moving average, *Aircraft Engineering and Aerospace Technology* 96:8 (2023) 1074–1082. doi: 10.1108/aeat-01-2023-0018.
- [19] C. Wang, X. Zhu, X. Zhou, J. Huang, F. Lu, Performance Monitoring Based on Improved Adaptive Kalman Filtering for Turboshift Engines Under Network Uncertainties, *Aerospace* 12:3 (2025) 241. doi: 10.3390/aerospace12030241.
- [20] A. D. Fentaye, K. G. Kyprianidis, An intelligent data filtering and fault detection method for gas turbine engines, *MATEC Web of Conferences* 314 (2020) 02007.
- [21] C. Manasis, N. Assimakis, V. Vikias, A. Ktena, T. Stamatelos, Power Generation Prediction of an Open Cycle Gas Turbine Using Kalman Filter, *Energies* 13:24 (2020) 6692.
- [22] S. Nandy, R. Singh, A. Maity, P. S. V. Nataraj, Robustification of Unscented Kalman Filtering to Identify Faults in Gas Turbine Engine, *IFAC-PapersOnLine* 55:1 (2022) 826–831.
- [23] M. Razmjooei, F. Ommi, Z. saboohi, Experimental analysis and modeling of gas turbine engine performance: Design point and off-design insights through system of equations solutions, *Results in Engineering* 23 (2024) 102495. doi: 10.1016/j.rineng.2024.102495.
- [24] X. Zhang, M. Zhong, K. T. Ooi, T. Zhang, Incipient instability real-time warning via adaptive wavelet synchrosqueezed transform: Onboard applications from compressors to gas turbine engines, *Energy* 308 (2024) 132925. doi: 10.1016/j.energy.2024.132925.
- [25] S. Ma, Y. Wu, H. Zheng, L. Gou, A Hybrid of NARX and Moving Average Structures for Exhaust Gas Temperature Prediction of Gas Turbine Engines, *Aerospace* 10:6 (2023) 496. doi: 10.3390/aerospace10060496.

- [26] D. Miao, K. Feng, Y. Xiao, Z. Li, J. Gao, Gas Turbine Anomaly Detection under Time-Varying Operation Conditions Based on Spectra Alignment and Self-Adaptive Normalization, *Sensors* 24:3 (2024) 941. doi: 10.3390/s24030941.
- [27] S. Vladov, Y. Shmelov, R. Yakovliev, Methodology for Control of Helicopters Aircraft Engines Technical State in Flight Modes Using Neural Networks, *CEUR Workshop Proceedings* 3137 (2022) 108–125. doi: 10.32782/cm137-10. URL: <https://ceur-ws.org/Vol-3137/paper10.pdf>
- [28] C. Hu, K. Miao, M. Zhou, Y. Shen, J. Sun, Intelligent Performance Degradation Prediction of Light-Duty Gas Turbine Engine Based on Limited Data, *Symmetry* 17:2 (2025) 277.
- [29] S. Vladov, A. Sachenko, V. Sokurenko, O. Muzychuk, V. Vysotska, Helicopters Turboshift Engines Neural Network Modeling under Sensor Failure, *Journal of Sensor and Actuator Networks* 13:5 (2024) 66. doi: 10.3390/jsan13050066
- [30] H. Zhou, Y. Ying, J. Li, Y. Jin, Long-short term memory and gas path analysis based gas turbine fault diagnosis and prognosis, *Advances in Mechanical Engineering* 13:8 (2021).
- [31] S. Vladov, A. Banasik, A. Sachenko, W. Kempa, V. Sokurenko, O. Muzychuk, P. Pikiewicz, A. Molga, V. Vysotska, Intelligent Method of Identifying the Nonlinear Dynamic Model for Helicopter Turboshift Engines, *Sensors* 24:19 (2024) 6488 doi: 10.3390/s24196488.
- [32] W. H. Chung, Y. H. Gu, S. J. Yoo, CHP Engine Anomaly Detection Based on Parallel CNN-LSTM with Residual Blocks and Attention, *Sensors* 23:21 (2023) 8746. doi: 10.3390/s23218746.
- [33] S. Vladov, L. Scislo, V. Sokurenko, O. Muzychuk, V. Vysotska, S. Osadchy, A. Sachenko, Neural Network Signal Integration from Thermogas-Dynamic Parameter Sensors for Helicopters Turboshift Engines at Flight Operation Conditions, *Sensors* 24:13 (2024) 4246.
- [34] I. Perova, Y. Bodyanskiy, Adaptive human machine interaction approach for feature selection-extraction task in medical data mining, *International Journal of Computing* 17:2 (2018) 113–119. doi: 10.47839/ijc.17.2.997
- [35] B. Rusyn, O. Lutsyk, R. Kosarevych, O. Kapshii, O. Karpin, T. Maksymyuk, J. Gazda, Rethinking Deep CNN Training: A Novel Approach for Quality-Aware Dataset Optimization, *IEEE Access* 12 (2024) 137427–137438. doi: 10.1109/access.2024.3414651
- [36] S. Vladov, Y. Shmelov, R. Yakovliev, Method for Forecasting of Helicopters Aircraft Engines Technical State in Flight Modes Using Neural Networks, *CEUR Workshop Proceedings* 3171 (2022) 974–985. URL: <https://ceur-ws.org/Vol-3171/paper70.pdf>
- [37] S. Vladov, Y. Shmelov, R. Yakovliev, M. Petchenko, S. Drozdova, Neural Network Method for Helicopters Turboshift Engines Working Process Parameters Identification at Flight Modes, in: *Proceedings of the 2022 IEEE 4th International Conference on Modern Electrical and Energy System (MEES)*, Kremenchuk, Ukraine, 20–22 October 2022, pp. 604–609.
- [38] M. Komar, A. Sachenko, V. Golovko, V. Dorosh, Compression of network traffic parameters for detecting cyber attacks based on deep learning. In *Proceedings of the 2018 IEEE 9th International Conference on Dependable Systems, Services and Technologies (DESSERT)*, Kyiv, Ukraine, 2018, pp. 43–47. doi: 10.1109/DESSERT.2018.8409096
- [39] S. Babichev, J. Krejci, J. Bicanek, V. Lytvynenko, Gene expression sequences clustering based on the internal and external clustering quality criteria, in: *Proceedings of the 2017 12th International Scientific and Technical Conference on Computer Sciences and Information Technologies (CSIT)*, Lviv, Ukraine, 05–08 September 2017.
- [40] N. Shakhovska, V. Yakovyna, N. Kryvinska, An improved software defect prediction algorithm using self-organizing maps combined with hierarchical clustering and data preprocessing. *Lecture Notes in Computer Science* 12391 (2020) 414–424. doi: 10.1007/978-3-030-59003-1_27.
- [41] Z. Hu, E. Kashyap, O. K. Tyshchenko, GEOCLUS: A Fuzzy-Based Learning Algorithm for Clustering Expression Datasets, *Lecture Notes on Data Engineering and Communications Technologies* 134 (2022) 337–349. doi: 10.1007/978-3-031-04812-8_29.
- [42] R. M. Catana, G. Dediu, Analytical Calculation Model of the TV3-117 Turboshift Working Regimes Based on Experimental Data, *Applied Sciences* 13:19 (2023) 10720.
- [43] S. Vladov, M. Bulakh, V. Vysotska, R. Yakovliev, Onboard Neuro-Fuzzy Adaptive Helicopter Turboshift Engine Automatic Control System, *Energies* 17:16 (2024) 4195.

- [44] W. Du, J. Zhang, G. Meng, H. Zhang, Aero-Engine Fault Detection with an LSTM Auto-Encoder Combined with a Self-Attention Mechanism, *Machines* 12:12 (2024) 879.
- [45] G. Qu, T. Qiu, Y. Si, Q. Yuan, Q. Ma, C. Wang, Remaining Useful Life Prediction for Aero-Engine Based on Hybrid CNN-GRU Model, in: *Proceedings of the 2022 IEEE International Conference on Unmanned Systems (ICUS)*, Guangzhou, China, 28–30 October 2022, pp. 1523–1528. doi: 10.1109/icus55513.2022.9987018.
- [46] U. Thakkar, H. Chaoui, Remaining Useful Life Prediction of an Aircraft Turbofan Engine Using Deep Layer Recurrent Neural Networks, *Actuators* 11:3 (2022) 67. doi: 10.3390/act11030067.
- [47] S. Ablamskyi, O. Muzychuk, E. D’Orio, V. Romaniuk, Taking biological samples from a person for examination in criminal proceedings: correlation between obtaining evidence and observing human rights, *Revista de Direito Internacional* 20:1 (2023).
- [48] S. Tovkach, Middleware Service for the Integration of Control Systems of the Aviation Engine and Aircraft, in: A. Bieliatynskiy, V. Breskich, (eds), *Safety in Aviation and Space Technologies. Lecture Notes in Mechanical Engineering*. Springer, Cham. doi: 10.1007/978-3-030-85057-9_2.
- [49] A. R. Marakhimov, K. K. Khudaybergenov, Approach to the synthesis of neural network structure during classification, *International Journal of Computing* 19:1 (2020) 20–26. doi: 10.47839/ijc.19.1.1689.
- [50] A. Berko, V. Aliksieiev, V. Holdovanskyi, Determination-based correlation coefficient, *CEUR Workshop Proceedings* 3711 (2024) 198–224. URL: <https://ceur-ws.org/Vol-3711/paper12.pdf>
- [51] M. Pasioka, N. Grzesik, K. Kuźma, Simulation modeling of fuzzy logic controller for aircraft engines, *International Journal of Computing* 16:1 (2017) 27–33. doi: 10.47839/ijc.16.1.868
- [52] I. Perova, Y. Bodyanskiy, Adaptive human machine interaction approach for feature selection-extraction task in medical data mining, *International Journal of Computing* 17:2 (2018) 113–119. doi: 10.47839/ijc.17.2.997.
- [53] V. Kovtun, T. Altameem, M. Al-Maitah, W. Kempa, Entropy-Metric Estimation of the Small Data Models with Stochastic Parameters, *Heliyon* 10 (2024) e24708. doi: 10.1016/j.heliyon.2024.e24708.
- [54] A. Urooj, S. Elferik, Adaptive Particle Swarm Optimization based Self-Tuning Control for Combustion Engines. *Transportation Research Procedia* 84 (2025) 97–104.
- [55] N. Shakhovska, R. Kaminsky, E. Zasoba, M. Tsiutsiura, Association rules mining in big data, *International Journal of Computing* 17:1 (2018) 25–32, 2018. doi: 10.47839/ijc.17.1.946.
- [56] G. Stamatescu, I. Făgărășan, A. Sachenko, Sensing and Data-Driven Control for Smart Building and Smart City Systems, *Journal of Sensors* 2019 (2019) 1–3. doi: 10.1155/2019/4528034.
- [57] V. Inzillo, F. De Rango, A. Ariza Quintana, A low energy consumption smart antenna adaptive array system for mobile ad hoc networks, *International Journal of Computing* 16:3 (2017) 124–132. doi: 10.47839/ijc.16.3.895.
- [58] O. Shapoval, R. Vakulenko, V. D. Kulynych, I. V. Savchenko, Tube Sheet Ligament Thickness Selection and Stress Analysis during Tube Expansion, *Key Engineering Materials* 1004 (2024) 85–91. doi: 10.4028/p-h2x9di.
- [59] L. Karpukov, V. Voskoboynik, I. Savchenko, O. Parshyna, O. Shapoval, V. Piven, Optimal Synthesis of Band-Pass Filters on Coupled Microstrip Lines, in: *Proceedings of the 2024 IEEE 7th International Conference on Smart Technologies in Power Engineering and Electronics, STEE 2024*, Kyiv, Ukraine, 24–26 September 2024.
- [60] J. Rabcan, V. Levashenko, E. Zaitseva, M. Kvassay, S. Subbotin, Application of Fuzzy Decision Tree for Signal Classification, *IEEE Transactions on Industrial Informatics* 15:10 (2019) 5425–5434, Oct. 2019. doi: 10.1109/tii.2019.2904845.